Contemporary Physics, 1995, volume 36, number 2, pages 79–92

Computer modelling of violin playing

R. T. SCHUMACHER† AND J. WOODHOUSE‡

In the last 15 years there has been significant progress in the understanding of the oscillations of musical instruments. This progress comes in part from the increased understanding of the basic physical mechanisms involved in the oscillations, but some of the major successes arise from a successful adaptation of the physical models to rapid computer calculation of the waveforms of oscillation. In this article we review research on the bowed string, where computation speed is now allowing a fruitful exploration of the enormous parameter space needed to describe the instrument, its strings and the string player's control of them in a musical context.

1. Introduction

Many scientists are intrigued by the facts and folklore surrounding the violin, and this curiosity goes back as long as there have been scientists. How does it happen that certain violins can command astronomical prices, while others, superficially similar, can be bought for a price which is lower by a factor of 10^4? Why does it seem not to be possible to duplicate the performance of the famous old instruments, given the advances in both theoretical and experimental techniques for studying sound and vibration? Unfortunately, when one makes a serious effort to apply these techniques, one finds time and again that one is pushing against the limits of what can yet be achieved.

The main reason for this is that the violin, in common with any other successful musical instrument, has evolved to take best advantage of human abilities; it allows motor actions up to the limit of what we can achieve to be turned into a range of sounds which we can process most acutely. This double optimality makes musical acoustics a more demanding discipline than other branches of acoustics. One is frequently confronted with rather subtle physical effects which result in sounds that our auditory system happens to be able to process with astonishing acuity. It is never safe to assume that, because a particular effect is small in terms of physical measurements, it will therefore not be significant to a skilled musician.

In barest outline, the chain of events which takes place when a violin is played is easily described. One of the strings of the instrument is set into vibration by the frictional action of drawing the bow across it, and the precise form of the vibration is controlled by the player through the bowing gesture and the actions of the left-hand fingers in stopping the string to the correct pitch and providing vibrato. A vibrating string on its own generates virtually no radiated sound (because its diameter is very small compared with the wavelength of sound in air in the relevant frequency range); so an amplification device is needed. The transverse vibration of the tensioned string applies an oscillatory force to the point of the violin bridge where the string makes contact. This force sets the bridge, and hence the wooden violin body upon which it rests, into vibration. The dimensions of the body are of the same order of magnitude as acoustic wavelengths, and relatively efficient sound generation is the result. The particular violin body will impart something of its own character to the sound at this stage; the resonances of the structure will produce a particular distribution of enhanced and suppressed frequencies. The radiated sound waves then interact with the acoustical behaviour of the auditorium, and finally reach the ears of the listener. They also reach the player's own ears, allowing a feedback process to operate in which the details of playing are modified if the sound is unsatisfactory.

The most reliable judgments of violins, when seeking to pin down physical correlates of 'quality', are obtained not from listeners but from players. By the feedback process just mentioned, a good player may be able to make compensations which mask the inadequacies of a poor instrument to a considerable extent, so that a listener is hardly aware of them. (A typical anecdote to this effect appears in the recent memoirs of André Previn [1], relating to a master class given by Jascha Heifetz; a student tried to lay the blame for her poor tone on an inferior instrument, whereupon the master took it from

†*Author's address:* Department of Physics, Carnegie Mellon University, Pittsburgh, Pennsylvania 15213, USA.
‡*Author's address:* Cambridge University Engineering Department, Trumpington Street, Cambridge CB2 1PZ, England.

0010-7514/95 $10·00

her and demonstrated otherwise.) However, the player, being inside the feedback loop of those compensations, will still be quite well aware that the instrument is poor, precisely because it calls for such compensation: it is unlikely that Heifetz offered to buy the student's violin. This suggests that physical correlates be sought for differences of 'playability' between instruments. Such differences certainly exist, and they point to the possibility that the stick–slip oscillations produced by bowing a string are somehow influenced in their details by the acoustical behaviour of the wooden box which is the violin body, to which the string is attached.

These are matters suitable for investigation by the physicist. Theoretical and experimental study of the bowed string has a long history, and the physical basis for much of the observed behaviour is believed to be fairly well understood. A bowed string is a self-sustained oscillator, in which a complicated linear system (the string, with attached violin body, which is in turn weakly coupled to the acoustics of the auditorium) is driven by the frictional force from the bow. This frictional force is strongly nonlinear in its dependence on the string motion under the bow. This description is generically similar to that of various other nonlinear systems which have been much studied in recent years, so that complicated behaviour involving the possibility of many periodic and non-periodic ('chaotic') regimes might be anticipated. That expectation is in qualitative agreement with the wide range of unmusical noises that can be elicited from a violin, especially in the hands of a novice. Computer studies based on theoretical models of bowed strings are beginning to provide quantitative information. Although such studies are in their infancy some interesting results have been obtained, and the purpose of this article is to review them.

2. Regimes of bowed-string oscillation

The violinist is almost always trying to achieve a particular regime of string oscillation, one that was first described by Helmholtz [2] and is thus known as 'Helmholtz motion'. It is a periodic, or (in practice) at least approximately periodic, regime [3, 4] in which the string sticks to the bow for most of the time, slipping rapidly backwards relative to the bow motion just once per vibration period. Many issues of 'playability' depend on how the detailed form of the Helmholtz motion can be modified by the player to produce variations in tone colour, and on how readily Helmholtz motion can be initiated and maintained using the various different bowing techniques which a player wants to be free to choose for musical reasons.

The idealized form of this Helmholtz motion is illustrated in figure 1(*a*). It is approximately a free motion of the string, in which a rather sharp 'corner' shuttles back and forth around the visible envelope of the string vibration. As the corner passes the bow, it triggers transitions between sticking friction and sliding friction, and vice versa. The result is a velocity waveform at the bow like that shown in figure 1(*b*), with one episode of slipping and one of sticking in every cycle. The role of the bow is to supply sufficient energy during the sticking phase to compensate for any energy losses to sound radiation and internal dissipation in the string, bow or instrument body. The geometry of the Helmholtz motion dictates that the length of slipping time as a fraction of the cycle period is equal to the fractional distance of the bowed point along the length of the string. This is conventionally designated β; if the string length is L, the bowed point is a distance βL from the bridge. In normal violin playing, β takes quite small values, perhaps in the range 0·2–0·02, more extreme values being used for special effects.

When the string is executing a Helmholtz motion, the (small) angle between the string and the direction normal to the bridge changes monotonically throughout the cycle, except for the moment at which the corner reflects from the bridge, when this angle jumps. It follows that the waveform of transverse force applied by the string to the bridge is a sawtooth, as shown in figure 1(*c*). An interesting consequence is that the driving waveform for the instrument body is, to a first approximation, independent of almost everything the player can control: for example the type of string, and the bow force (i.e. the force with which the bow is pressed against the string). Only the amplitude of the force waveform varies with the parameters controlled by the player in steady bowing; it scales linearly with bow speed and inversely with β and a player controls loudness primarily by a balance between these two quantities.

The actual force waveform in practice usually approximates the sawtooth quite closely. A typical example is shown in figure 1(*d*), measured on the open A string of a cello using a piezoelectric force transducer built into the top of the bridge. Any variation in tone colour which a player can produce must arise from the (small) departures of this waveform from the ideal sawtooth form, and (much more importantly) from the variety of initial transients which can be created by different bowing gestures. One instrument will differ from another in sound because of the different resonance and radiation characteristics of their soundboxes, and also they may differ in 'playability' because the transient response of the strings to bowing might be influenced by the different body responses at the string terminations. This latter possibility is the long-term goal of the study reported in this article. Computer simulation can be used to investigate whether current theoretical models of the bowed string predict sensitivity of transient behaviour to various parameters of the instrument, string and player's bowing gesture. Work so far has focused mainly on the last two of these three items.

Several periodic regimes besides the Helmholtz motion are often encountered, both on real strings and in computer simulations. They are of interest here since they represent

ways that a Helmholtz motion might break down or fail to be established from an initial bowing transient. In a pioneering study of bowed-string motion, Raman [6] gave an ingenious kinematic argument which showed that *all* periodic motions of a bowed string might be expected to exhibit travelling 'corners' of the Helmholtz type. Raman developed a classification of the possible periodic oscillation regimes in terms of the number of corners on the string which they entail. The Helmholtz motion is in these terms the simplest oscillation, with only one corner. Other regimes, called by Raman 'higher types', involve larger numbers of corners. Raman's classification seems to work well for most regimes encountered in practice, although examples are sometimes encountered which are not easy to fit into his scheme and which are the subject of continuing research.

We illustrate the bridge-force waveforms associated with some important regimes, all recorded on the same cello string as figure 1(*d*). First is the 'double-slip motion'. If the bow force (controlled directly by the player) is insufficiently high, it is not possible for the string to stick to the bow throughout the nominal sticking period of the Helmholtz motion. A second slip occurs, usually near the middle of the 'sticking' period. The bridge-force waveform is then a 'double sawtooth wave', of which an example is shown in figure 2(*a*). Sometimes, the second slip grows to equal magnitude with the first, and the note may then sound an octave higher. More commonly the slips are of unequal magnitude and/or timing, so that the fundamental frequency is unchanged. The tone quality is significantly changed, however, and the result is usually described by string players as 'surface sound'. In terms of Raman's classification, this is motion of the second type, since it involves two travelling corners (as is immediately apparent from the bridge-force waveform).

The next type of motion, shown in figure 2(*b*), is less well known. There is a family of such motions, which have been named 'multiple flyback motions'. The waveform is still reminiscent of the Helmholtz sawtooth, except that the single 'flyback' of the Helmholtz motion has been replaced by a cluster of them, with alternating signs. The motion involves

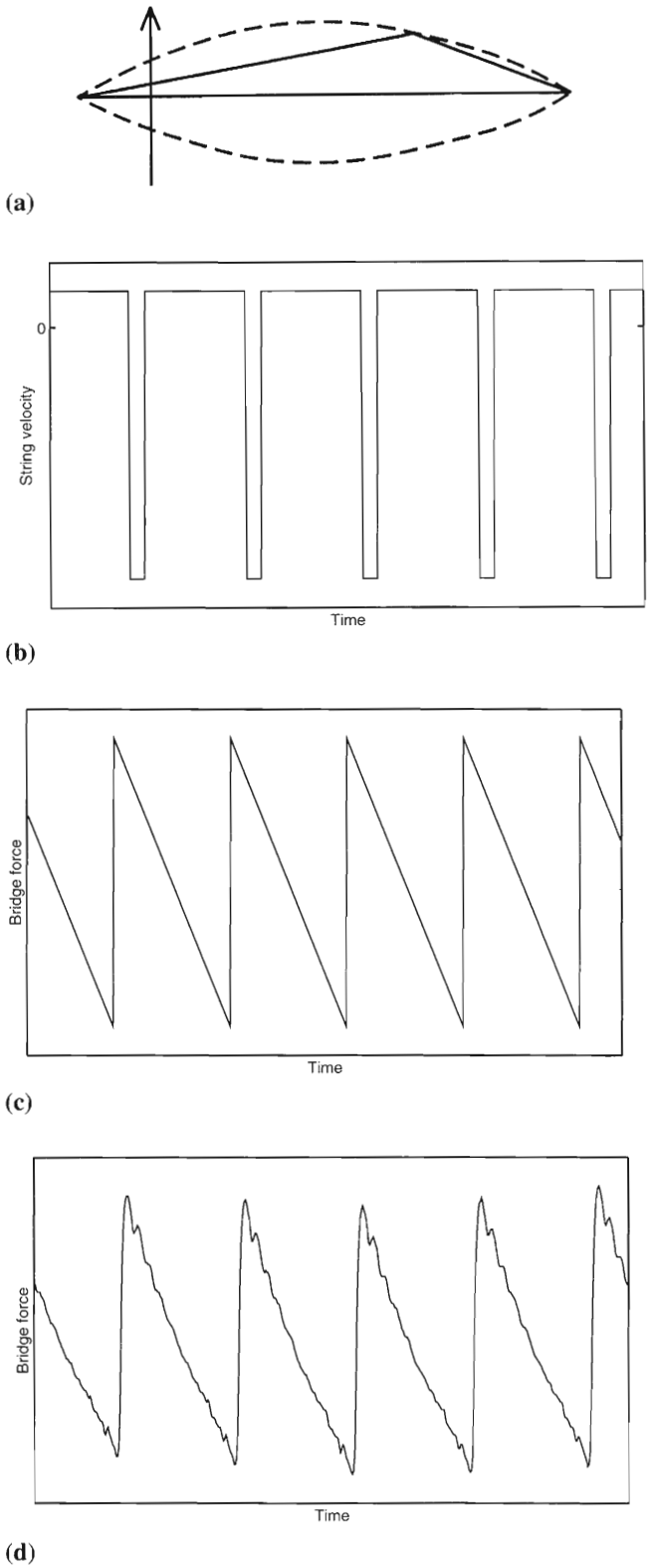

Figure 1. (a) The motion of a bowed string during the Helmholtz motion: (– – – – –) envelope of the string vibration; (———) 'snapshot' of a typical string position; and the arrow indicates the position and motion of the bow. (b) The waveform of string velocity at the bowed point during an ideal Helmholtz motion, showing an alternation between sticking and slipping during each period of the oscillation. (c) The waveform of transverse force exerted by the string on the bridge during an ideal Helmholtz motion. (d) Bridge force waveform measured on the open A string of a cello executing Helmholtz motion, showing a reasonable approximation to the sawtooth wave of (c). The most obvious difference in the two waveforms takes the form of 'wiggles' visible in this waveform, which arise when small perturbations to the motion reflect back and forth between the bridge and the bow during the sticking portion of the Helmholtz cycle. The quasiperiodicity of these so-called 'Schelleng [5] ripples' is associated with the position β of the bowed point on the string.

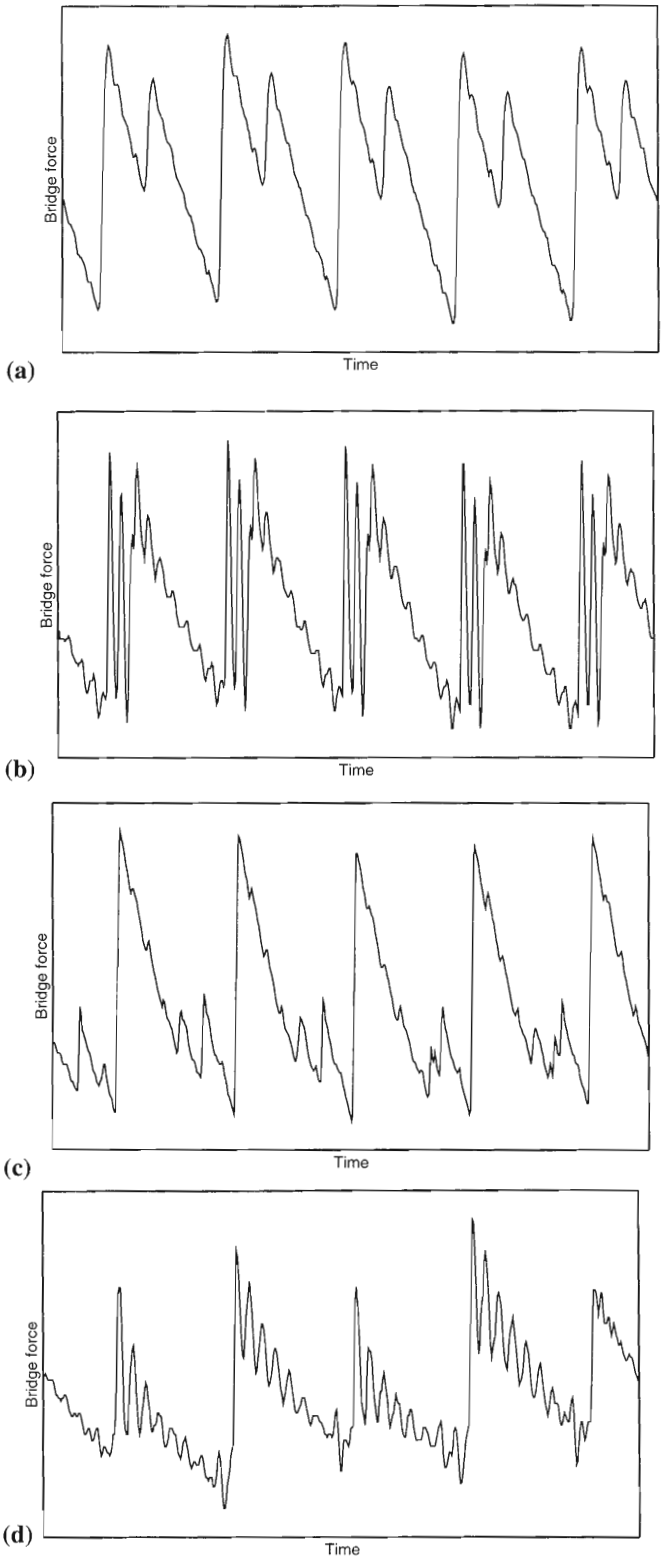

Figure 2. Bridge force waveforms for various oscillation regimes of the cello A string used in figure 1(d), with the same time scale as that figure: (a) double-slip motion, 'surface sound'; (b) multiple-flyback motion; (c) Helmholtz motion with 'spikes'; (d) irregular 'raucous' motion, obtained when the bow force is too high.

more than one slip per period but, instead of being spread through the whole period as in the 'surface sound', they also appear in a tight cluster. This regime is recognized by players as leading to an undesirable sound but has not been the subject of any detailed investigation. The example shown here is, in Raman's terms, a 'fifth type', since it involves five travelling corners. The second and fourth of the cluster of five have opposite signs, meaning that they are travelling around the string with the opposite sense. Closely related regimes are encountered with other numbers of 'flybacks' in the cluster: three, seven and higher (odd) numbers are seen in computer simulations, and cases involving three, five and seven have been observed in practice.

The other two examples of bridge-force waveforms shown in figures 2(*c*) and (*d*) show non-periodic oscillation regimes. Both arise when the bow force is high. If a Helmholtz motion is established on a given string and the bow force is slowly increased, something will eventually go wrong. At moderate force, one may notice the growth of an audible noise component accompanying the musical note. This is the case shown in figure 2(*c*); superimposed on the Helmholtz sawtooth waveform are small, irregularly spaced 'spikes'. These result from an effect of the finite width of the ribbon of bow hair: the spikes correspond to times when the string slips from some of the bow hairs (usually on the side of the bow nearer to the bridge), while continuing to stick to the remaining bow hairs [3, 7]. If the bow force is increased further, all semblance of musical note may be lost, leading to a raucous 'crunch'. The passage of the Helmholtz corner past the bow no longer exerts sufficient force to trigger a transition from sticking to slipping, so that the accurate timekeeping of the Helmholtz motion is lost. Usually, an aperiodic regime results, as shown in figure 2(*d*). With very careful control of the bow force a periodic note at a substantially lower pitch may sometimes be produced instead, a possibility which has recently excited some interest for its musical potential[8]. (For musical application see the review by Edward Rothstein of a concert by Mari Kimura [9].)

3. Theoretical models

To learn something about these regimes of oscillation, and to begin to attack the questions raised in the introduction, a theoretical model is needed. We shall describe briefly a model of bowed-string motion that seems to be the simplest which captures most of the essential physics, and which is capable of reproducing many qualitative phenomena that are observed in real violin strings. Surprisingly, closely related models can be applied to many wind instruments, but that issue is not explored here. The review article in [10] discusses the simplest versions of the corresponding clarinet and flute models.

The model assumes that the bow is applied at a single point on the string. At this bowed point there are two relevant

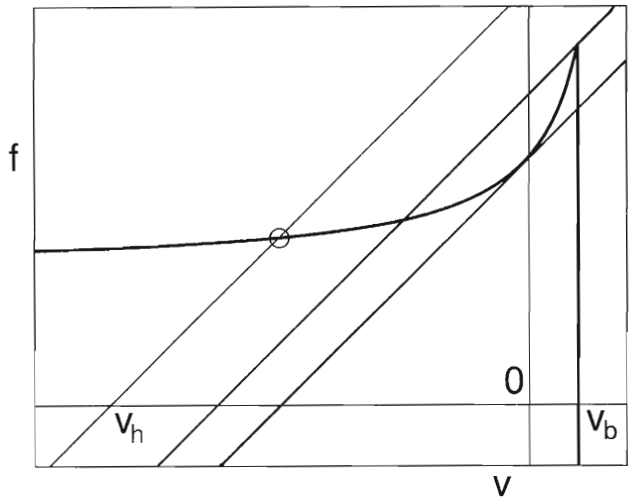

Figure 3. The bold curve shows the relation between the frictional force f and string velocity v at the contact point. The straight line and ringed intersection illustrate the approach to solving f(v) simultaneously with equation (1). The other two straight lines demarcate the limits of the ambiguous region for this solution, discussed briefly in section 4.

variables to consider, the frictional force $f(t)$ between bow and string and the transverse velocity $v(t)$ of the point on the string beneath the bow. These two quantities are related in two quite different ways, and the combination of the two gives rise to the model equations. First, the force and the velocity are related by the frictional properties of the rosin used to promote stick–slip vibration. The simplest model for this assumes a functional relation between the two variables, of the kind illustrated by the curve in figure 3. When the velocity of the string at the bowed point is equal to the speed v_b of the bow, then the two are sticking together and the frictional force can take any value between the limits set by the normal bow force F_b multiplied by the coefficient of sticking friction. This corresponds to the vertical portion of the curve. When there is relative motion between bow and string, there will be a sliding frictional force which is assumed to be a function of relative speed. The rheological properties of the rosin used to coat the hairs of the bow produce a variation like that shown in the figure. This simple model of friction suffices for our present purpose, although recent work [11,12] has suggested that a more realistic model should take account of the *thermal history* of the rosin near the contact point; there is some evidence that the rosin actually melts and resolidifies a little during each cycle of stick–slip oscillation.

The second mechanism relating the force to the velocity at the bowed point on the string is the linear vibration behaviour of the string and its attached hardware of instrument body and player's finger. If we apply any given force waveform $f(t)$ to a point on the string, a velocity response will be evoked. It consists of an immediate response to the force, together with the combined effect of all reflected waves arising from earlier forcing which happen to arrive back at the bowed point at that particular moment. It is convenient to divide the velocity response explicitly into these two components. The instantaneous response to force $f(t)$ is simply the response of an infinite string to the force (since an infinite string has no returning reflections). This response is $(Y/2)f(t)$, where Y is the wave admittance of the string (given for an ideal string by $Y = (Tm)^{-1/2}$, where T is the string tension and m its mass per unit length). The effect of returning reflected waves we shall denote $v_h(t)$, where the subscript h suggests 'history'. Thus

$$v(t) = \frac{Y}{2} f(t) + v_h(t) \tag{1}$$

It is now easy to see roughly how a time-stepping simulation of this model can be carried out. At a given time t, we can calculate the value of $v_h(t)$ because it depends only on previous history. We then solve simultaneously for the new values of $v(t)$ and $f(t)$, using the friction curve together with equation (1), which is the equation of a straight line. The required values are found at the intersection point, as illustrated in figure 3.

The major computational task at each time step is thus to calculate $v_h(t)$. The motion of the string immediately around the bow can be represented, at a reasonable level of approximation, by a superposition of transverse waves travelling to the left and to the right at the characteristic wave speed of the string. When we apply a force impulse at the bowed point, two identical impulses are launched, travelling outwards from that point. By considering the fate of these two impulses separately, we can obtain a prescription for $v_h(t)$ which is both computationally efficient and physically illuminating. The first arrival back at the bowed point is a reflection from the violin bridge, consisting of an impulse which will have been inverted on reflection, and slightly 'smeared' during its travel. A little later the first reflection returns from the other end of the string, after the longer journey to the violinist's finger and back. This will also have been smeared out, in a rather different way since it has had a longer journey on the string and has reflected from a different kind of termination.

We may represent these two reflection processes by two functions, with which the initial impulse must be convolved to produce the smeared pulses. The 'reflection function' for one half of the string is defined to be the impulse response at the 'bowed' point in the absence of the bow, when the other half of the string is replaced by a semi-infinite string from which no reflections ever return. These reflection functions will occupy a very much shorter time span than does the whole decay time of the string, so that computing convolution integrals with these function can be very fast. However, these short convolutions are all that we need calculate;

the subsequent reflections of the initial pulse, as the pulses travel back and forth past the bowed point, getting ever broader and slowly decaying away, are generated automatically. The mathematical details of this computationally-efficient model are given in appendix B of the paper by McIntyre *et al.* [10]. In summary, for each time step we need to perform two short convolutions with the two reflection functions, and then to calculate the point of intersection on the friction curve according to figure 3. That gives two new values of $v(t)$ and $f(t)$, and we are ready to proceed to the next time step.

The theoretical model of the string and violin body is thus encapsulated, as far as the bowing process is concerned, in the two reflection functions. These can be constructed in terms of more or less sophisticated physical models; to be fully realistic they must take into account the dissipation and dispersion which occurs as waves travel along the sections of the string, and also the reflection properties of the string terminations. Dissipation occurs through internal loss in the string material, dispersion arises from bending stiffness of the string, the vibration resonances of the instrument body determine the reflection behaviour at the violin bridge, and the physical properties of the player's finger govern the reflection at the other end of the string [13–15].

There is one further effect which needs to be taken into account in a realistic model. The frictional force is applied tangentially to the surface of the string, so that as well as exciting transverse waves it generates torsional waves. These also propagate along the string and generate reflections. The wave speed is generally higher than that for transverse waves [12, 13]. The combined propagation and reflection properties of torsional waves can be allowed for in a very similar way to that of transverse waves, with further reflection functions [10]. Although torsional waves in the string are probably not directly responsible for much of the sound from a violin, they play a very important role in the energy budget of the bowing process, and hence in determining the stability of bowed-string oscillation regimes [3, 13, 16]. Some supporting evidence for the importance of the torsional parameters of the string will be shown in the next section.

4. Simulation studies

A certain amount has been found out about bowed-string behaviour by analytical calculation, especially about which regimes of self-sustained oscillation are possible and stable under given conditions [5, 13, 16, 17], but the strongly nonlinear character of the system makes it hard to make any progress on questions of starting transients and of which of the possible regimes is actually chosen from a given bowing transient. Instead we turn to computer simulation, using the procedure just outlined. This simulation algorithm has been used to explore various questions of bowed-string behaviour, and it has also penetrated the commercial world (under the label 'physical modelling'), where musical synthesizers based on this technique are under development to replace or augment the FM-synthesis paradigm that has long dominated synthesizers and computer music [18].

Early implementations of the simulation algorithm took the form of interactive programs, in which the playing parameters could be varied during a run so that the program could be 'played', somewhat like the real string. Such computer experiments yielded many valuable insights into the bowing process and the strengths and weaknesses of the particular models used (for example Woodhouse [19]). However, the parameter space which one is exploring in this way is so large that it is extremely difficult to discern any structure in the overall behaviour from watching individual interactive runs of the program. To address the question of the robustness of Helmholtz motion to initial transients we can try to use simulations in a more systematic way, to map out some part of the player's parameter space and then to represent the results in pictorial form so that any interesting structure makes itself apparent. This strongly suggests that two-dimensional subspaces be identified for study, since it is hard to convey results in more than two dimensions.

The many parameters of the bowed-string problem can be grouped into three categories. The behaviour of the *instrument body* influences the string through the motion of the bridge. The constructional parameters of body and bridge are the concern of the maker of the instrument and the bridge, and to some extent may be adjusted by a violin repair shop. The *string's* characteristics are determined, but never very precisely specified, by the string maker. Finally we have the parameters of *playing*; the player chooses string length with the fingers of the left hand, and most importantly, controls the nature of the sound with the bow: its position on the string, its velocity, and the normal force exerted on the string. (We shall not here confront the additional problems of bow dynamics, involving issues such as where on the bow notes are initiated, and what the differences might be between individual bows.) We have done simulation studies based on a number of parameter 'planes' chosen from the latter two categories: string characteristics and bowing gestures. From this still very large-dimensional parameter space, we shall show examples of four different two-dimensional subspaces, chosen to highlight different aspects of behaviour.

To obtain a 'snapshot' of behaviour even in two dimensions, it is necessary to carry out, simultaneously or in sequence (depending on the computer resources available), a large number of simulations, each with its own values of the pair of parameters defining the plane. We display our results with coloured pictures containing from 3000 to 8192 pixels, one simulation per pixel, in the plane under study. To implement a systematic simulation scheme with such large numbers of cases it is necessary to be able to classify automatically the outcome of a particular transient, and in

particular to detect whether and when an acceptable Helmholtz motion becomes established. To do this, we use a detection criterion based on several simple tests. It is easy to test the oscillation for periodicity by computing the autocorrelation function. We also keep track of the number of stick–slip transitions, and the number of Raman 'corners' travelling on the string. The test for a successful Helmholtz oscillation is that the motion be acceptably periodic, and that the number of stick–slip transitions and the number of corners per period be equal to one. From the separate results for autocorrelation, number of slips and number of corners, it is also possible to make informed guesses about the nature of non-Helmholtz oscillations. Details of these tests have been described elsewhere [15, 20], where it is concluded that, while the scheme is not perfect, it appears to work well enough for the required investigation.

At a specified time after the start of the simulation, the set of tests just described can be applied and, if acceptable Helmholtz motion is found, the fact is recorded. The tests are repeated at set intervals of time, typically every five nominal periods. The results can then be represented in a plot in which colours are used to indicate the length of transient before Helmholtz motion is found, with black indicating pixels which never achieved Helmholtz motion within the total time simulated. Otherwise, a 'rainbow' palette is used, with red indicating the shortest transient, and purple the longest. Our typical runs are 100 nominal periods long, and the shortest initial transients that we have seen are over within the first five nominal periods.

For a first example, we choose a parameter plane aimed at quantifying a player's feeling that a given note might be either 'safe' or 'unreliable'. One bowing gesture may produce a Helmholtz motion quickly, but for an unreliable note another gesture, slightly different, might produce a different oscillation regime or have an unacceptably long transient. A range of somewhat plausible bowing transients can be constructed by varying just the imposed time history of the bow force; we allow the bow force to start from a specified value and to tend asymptotically to a different value, with an exponential decay of the difference. If the force starts from zero and increases to the final level, this gives a simple representation of a string-crossing transient in which the bow alights on the string and the force takes a finite time to build up. If the initial force is the same as the final value, a switch-on transient is produced. This probably does not represent anything done in normal playing, but it is a favourite condition for previous simulations and makes a useful comparison. If the force starts high and decreases to the final value, then we have at least a crude representation of a martelé transient (in which a player 'digs in' with the bow initially and then rapidly decreases force while increasing bow speed). An example of a fairly fast starting transient obtained from one of the cases, a 'martelé', is shown in figure 4. The bridge force for the first few nominal period lengths is shown. A recognizable Helmholtz sawtooth waveform is achieved at about nominal period 8.

We may now define a two-dimensional subspace of the 'bowing gesture' category by varying the initial force as one dimension, and the asymptotic value of the force as the other. The exponential time scale, and all other aspects of the model, including the bow velocity, are kept constant. An example of the output is shown in figure 5(*a*). The horizontal axis shows the asymptotic bowing force, on a logarithmic scale. The vertical axis shows, on a linear scale, initial force as a multiple of asymptotic force; at the bottom of the figure the initial force is zero, and at the top of each column of pixels the initial force is twice the asymptotic force specific to that column. The force begins as the specified multiple of the asymptotic force, and decays to the asymptotic force with an e-fold time of about four nominal periods. The model used for the rest of the system is the very simple model developed by Cremer [13], with additional features to allow for string anharmonicity, and for torsional behaviour of the string. The model allows, in a way appropriate to a violin string, for the frequency-dependent energy dissipation of both transverse [14, 20] and torsional [20, 21] waves on the string, but it does not model the reactive resonant nature of the response of the violin body. By separating string properties from body properties, we produce a very useful benchmark case against which the changes produced by more sophisticated models may be judged.

Three types of different non-Helmholtz behaviour (i.e. black pixels) can be distinguished, and these correspond well, qualitatively at least, to what happens in real playing. At a low asymptotic bow force, on the left of the picture, the Helmholtz motion gives way to other periodic regimes with more than one slip per period, 'surface sound'. At very high bow forces the coloured region has a rather fully vertical boundary. Beyond this, the asymptotic bow force is high

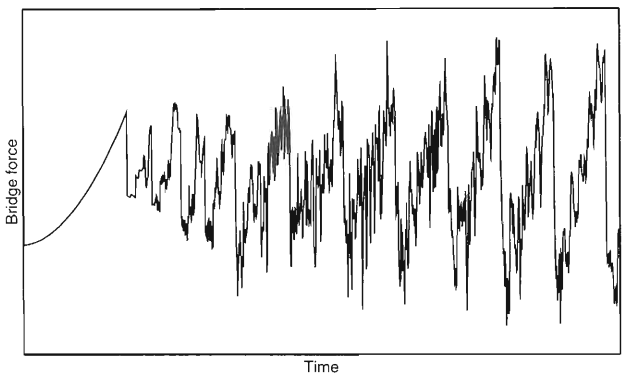

Figure 4. A typical example of the bridge-force waveform from a simulated 'martelé' bowing transient. A somewhat irregular Helmholtz sawtooth waveform can be seen in the final third of the time range plotted, and this soon settles to an accurately periodic state. The relatively high initial bow force produces a clearly visible delay before the first slip occurs.

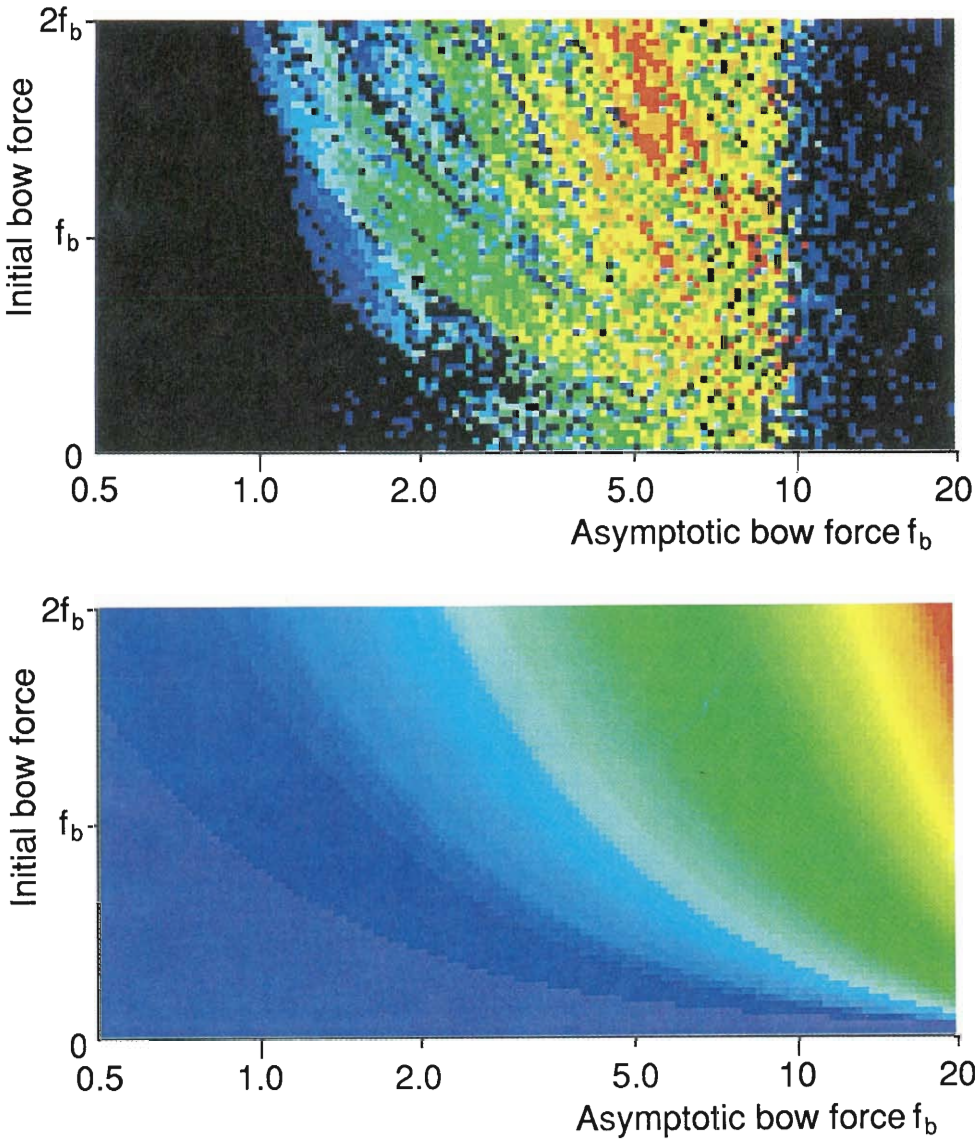

Figure 5. (a) Initial bow force against asymptotic bow force. The 128 horizontal pixels represent the asymptotic bow force, on a logarithmic scale. The bow force varies from 0·5 to 20 in units, used in all simulations, such that Y = 2. The vertical columns, 64 pixels long, represent the initial bow force, initially zero at the bottom, to twice the asymptotic bow force at the top. The colour scale is such that red signifies that Helmholtz motion has been achieved within 10 nominal periods, and purple that it has been achieved only between nominal period 90 and 95 of the 100 period run. Black indicates that Helmholtz motion was not achieved within 100 nominal periods. (b) Time to first slip in the same plane as (a). The rainbow palette indicates relatively short times on the lower left, increasing to the longest times on the upper right. See text for significance of contours of constant colour, which are widely spaced towards the lower left, more closely spaced at the upper right.

enough that periodic motion of any kind is not usually established. In between is a large area of coloured space liberally spotted with black or long-transient purple, which sometimes forms a discernible pattern of descending streaks. Helmholtz motion is established for most 'bowing gestures' in this region, except that the black pixels reveal the presence of a quite different periodic oscillation regime, 'multiple-flyback motion', which was described earlier. The fact that multiple-flyback motion is intermingled in the same region of parameter space as Helmholtz motion is in qualitative agreement with observations of the occurrence of this regime in practice.

A clue to the origin of the pattern of descending curves, which often seem to characterize lines of similar transient behaviour, is given by figure 5(*b*). Each simulation in figure 5(*a*) starts with the string at rest, and the bow hair and string

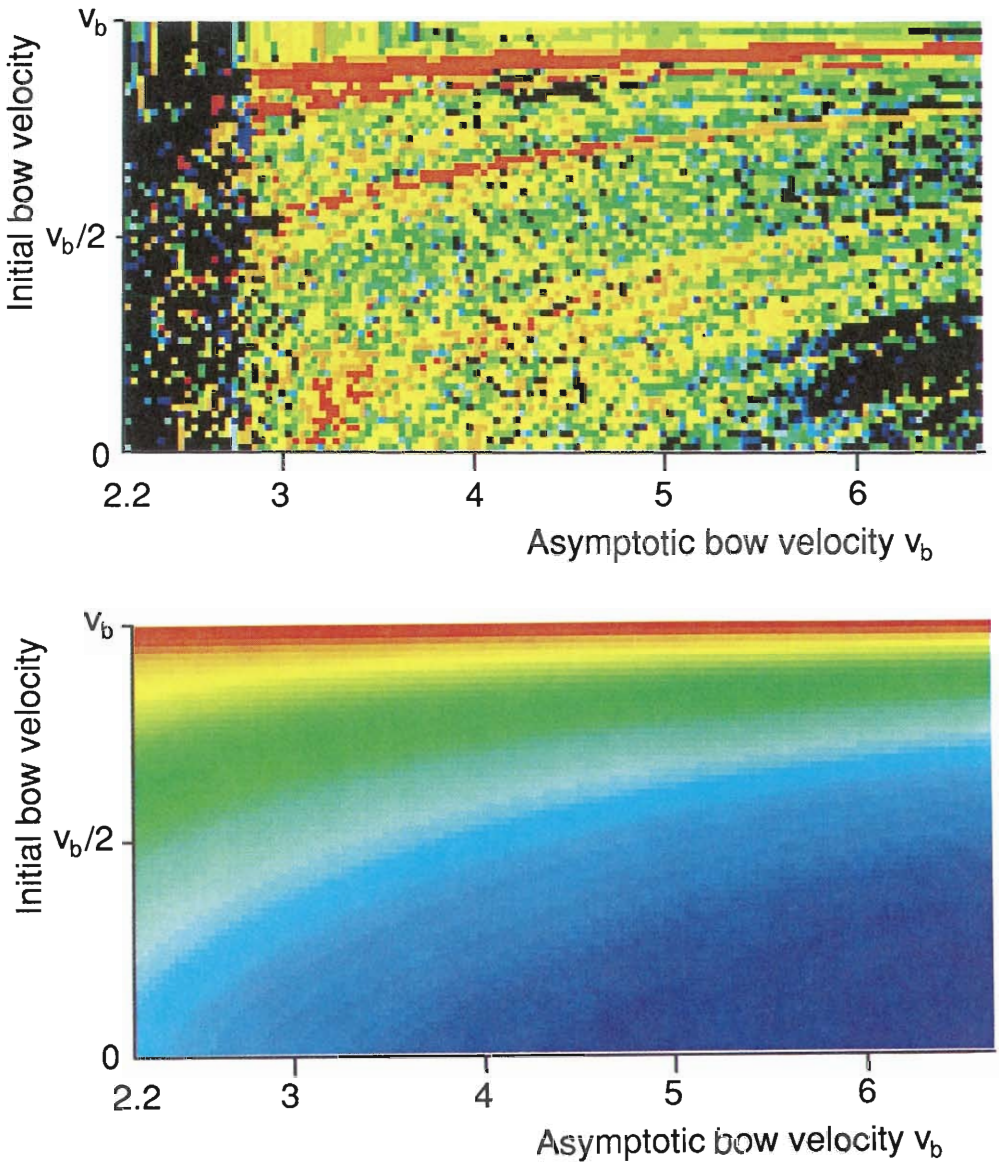

Figure 6. (a) Transient length for Helmholtz motion in a plane with axes initial bow velocity against asymptotic bow velocity. The colour palette has the same scale for transient length as in figure 5 (a). As in figure 5, there are 128 pixels (horizontal) by 64 pixels (vertical). (b) Time to first slip. As in figure 5(b), the contours of constant colour are widely spaced in the blue (short time to first slip) part of the figure, closer together in the red end.

sticking together. Figure 5(*b*) shows a similarly colour-coded plot of the time between simulation initiation and the first slip of the string relative to the bow hair, obtained from the same set of simulations that produced figure 5(*a*). There is quantitative agreement between the curves of constant time to first slip in figure 5(*b*) and the shapes of identifiable curves of similar transient length in figure 5(*a*). It appears that perhaps some critical event occurs very early in the transient, which strongly influences the eventual outcome and the transient length. However, it is as yet far from clear just how such a mechanism might operate, since the initial transients are in general long and (apparently) irregular between the first slip and the eventual steady oscillation. Even the rather short transient shown in figure 4 illustrates this irregularity.

A similar clue to the structural features of a bowing gesture can be seen in figure 6, in which a somewhat different subspace of gestures is explored. This time we allow time-varying bow speed, rather than bow force. This is done in a similar way to the previous case, so that the two parameters defining the plane are the asymptotic bow velocity (horizontal linear scale) and the initial bow velocity (vertical scale). The latter varies exponentially from an initial

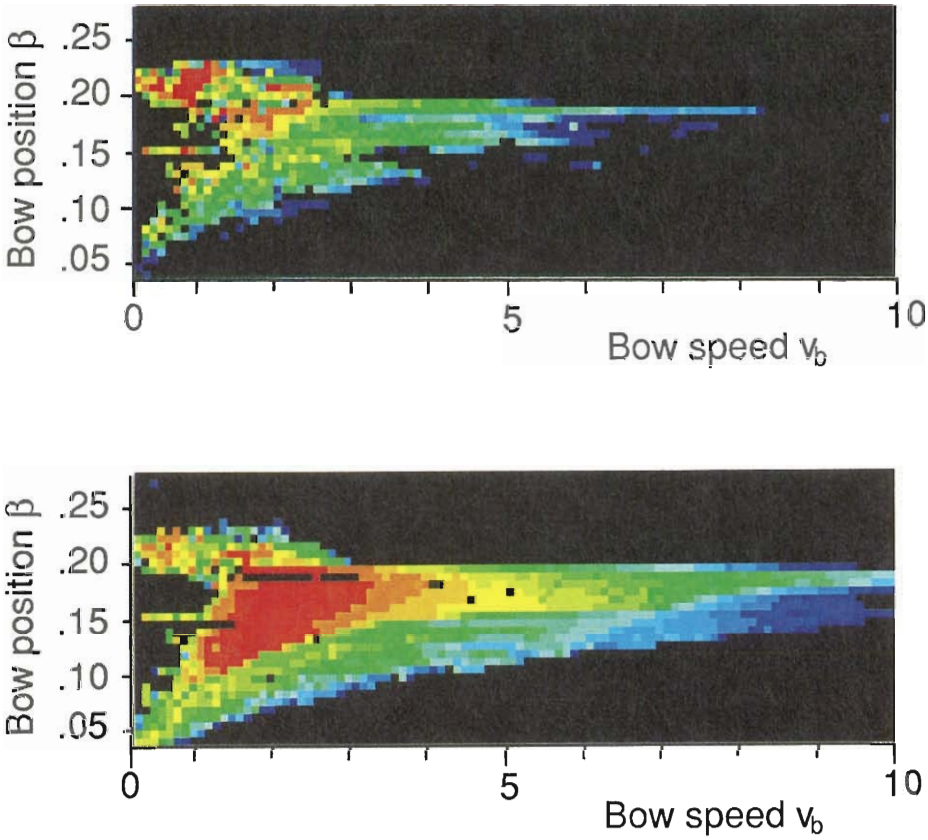

Figure 7. (a). The plane of bowing position against asymptotic bow velocity (98 pixels horizontal by 35 vertical). The bowing position is given in terms of the fractional distance β of the bowing point from the bridge. The reddest pixels mean here that Helmholtz motion has been achieved within the first five nominal periods. The bow velocity and bowing force are constant for each pixel, corresponding to the upper row of figure 6(a) and row 21 (counting from the bottom) of figure 5(a). (b) As (a), but with an initial sinusoidal disturbance on the string (see text for details).

velocity to the asymptotic bow velocity with a time constant of about three nominal periods. The initial bow velocity varies linearly from zero (bottom row) to the asymptotic velocity (top row); that is, in the top row the bow speed is constant throughout the transient. In all cases the bow force is held constant. As with figure 5, this family reproduces some of the features of bowing gestures used in practice.

The results tell a similar story to those in figure 5(*a*). The left-hand side of figure 6(*a*), with a low asymptotic bow velocity, corresponds qualitatively to the right-hand side of figure 5(*a*); in very broad terms, bow force and bow velocity need to be varied in tandem, so that if the bow velocity is reduced too far while the force is not, the force will be left too high for the prevailing velocity and non-periodic motion is likely to occur. In fact, figure 6(*a*) would look quite reminiscent of a portion of figure 5(*a*) if both axes were reversed. Figure 6(*a*) again reveals curves of similar transient length that, particularly for the shortest transients, prove to be identical in shape with lines of constant time to first slip, as shown in figure 6(*b*).

One bowing parameter at a violinist's disposal is the distance between bow and bridge, which is usually expressed in terms of the fractional distance β of the bow from the bridge. The proper management of this distance, in conjunction with bow velocity and bow force, is central to the violinist's bowing technique. In one of the earliest and most influential papers on player–instrument interaction, Schelleng [5] used a simple model of the string and its interaction with the body of the instrument to derive relations between bow force, position and speed that served as boundaries in that three-dimensional space for the existence of Helmholtz motion. Some of our most recent explorations of the space of bowing gesture have explored this 'Schelleng space'.

As an example, figure 7(*a*) shows the bowing distance β, varying linearly on the vertical axis, against bow velocity, on the horizontal axis. Helmholtz motion is found within a roughly triangular region. The region below the curved lower boundary of the coloured region corresponds

to a violation of the minimum bow force requirement, below which multiple slips occur, as in the left part of figure 5(*a*). The black region on the left-hand side of the figure corresponds to exceeding the maximum bow force for all the velocities in that region, and the waveforms becomes non-periodic. The shapes of these boundaries may be compared with Schelleng's formulae; he predicts that, at the 'minimum force' condition, $v_b \propto \beta^2$, which gives a qualitatively similar shape of boundary to that seen here while, at the 'maximum force' condition he predicts that $v_b \propto \beta$, which is not a very convincing description of what we see here. Schelleng's predictions for maximum bow force have been compared with experimental results and with simulations in a recent study [12], and his predictions for minimum bow force have been discussed in some detail in another study [15]. Improving on the understanding which underlies Schelleng's formulae is one of the targets of simulation studies such as those just shown.

The final boundary of the coloured region in figure 7(*a*) reveals a different phenomenon. The black region in the upper part of the figure shows a failure to establish Helmholtz motion when β is too large. This is in qualitative agreement with the experience of players; non-Helmholtz sounds are deliberately employed for certain colouristic effects by playing *sul tasto*, in other words with the bow rather far from the bridge, over the violin's fingerboard. In this region various of Raman's 'higher types' occur more readily than the Helmholtz motion. These simulation results give the first theoretically based characterization of the boundary of this region.

Figure 7(*a*) shares one feature in common with figures 5(*a*) and 6(*a*) that has not so far been commented upon. The coloured regions, presumably in some sense 'safe' for the player, are in fact mottled in their appearance; frequently, nearest-neighbour pixels have quite different transient lengths. Some of this variegation may be attributed to the vagaries of automatic recognition of an acceptable Helmholtz regime, but the qualitative phenomenon is undoubtedly real. It probably indicates a kind of sensitive dependence familiar from chaotic nonlinear systems (the 'butterfly's wingbeat effect').

A plausible mechanism for such behaviour has been advanced [20], based on the detailed behaviour of the construction shown in figure 3 for finding the appropriate values of $v(t)$ and $f(t)$ from the friction curve and the value of v_h. It is clear for the friction curve plotted in figure 3 that, for a certain range of v_h, the straight line and the friction curve have three intersections rather than a single intersection. A hysteresis cycle then results [10, 22], involving rapid 'jumps' when v_h passes through and out of the ambiguous region (in either direction). Now suppose that, at some point in a particular transient, v_h comes close to one of these 'jump' points and then turns back. A very slightly different transient, in contrast, might go through the 'jump' value. Thereafter the two solutions will have quite different character (one will have sticking at the contact, and the other slipping) and the subsequent evolution of the two need not come back together again.

String players are very sensitive to the problems of achieving reliable short transients, and are more so the lower the pitch of the instrument. One of the distinguishing features of an expert player is the ability to play cleanly even very rapid passages with multiple bow changes. A standard trick, used particularly by cellists, is to ensure that there is a disturbance present on the string before the bow transient is executed. One often catches cellists 'in the act', discreetly plucking a note with the left hand just before initiating the bowing gesture. It is an interesting test of the simulations to see whether such a disturbance, already present on the string, can change the appearance of pictures such as figure 7(*a*). Figure 7(*b*) shows the results of a run with the same parameters as figure 7(*a*), but with the addition of a sine wave of period equal to the nominal period of the bowed note in the initial conditions for each simulated run. The amplitude of the sine wave is constant over figure 7(*b*); amplitude is 5 in the units, used in all simulations, such that $Y = 2$, where Y is the wave admittance of the string as before. For scale comparison, an estimate of the magnitude of the Helmholtz jump in string velocity varies from about unity in the lower left to 4.0 in the upper right of figure 7. One sees in figure 7(*b*) that there are much larger contiguous regions of equal or neighbouring colour (in the rainbow sense), and that the region of shortest transient, confined to a single pixel in figure 7(*a*), has expanded to several dozen pixels. Examination of the waveforms in these very short transients (not reproduced here) shows that from the very beginning the disturbance predisposes the system to slip regularly every nominal period, so that a Helmholtz pattern is very quickly established. Also, the 'Helmholtz' region is now larger, mainly through a shift in the lower boundary; 'surface sound' occurs significantly less readily with the sinusoidal initial disturbance on the string.

We now turn to our final subspace of bowing parameters, one under the control of the string manufacturer. Strings are sold with all manner of core materials, around which wrappings, typically of aluminium or silver, may be coiled. Some strings are homogeneous; violin E strings are usually of steel, although are occasionally aluminium wrapped, and lower strings, particularly A and D, are available as homogeneous sheep gut without wrapping. By the choice of materials and constructional method, the manufacturer controls the linear mass density, the radial distribution of mass density, and the string's bending stiffness. These quantities may potentially influence the playing behaviour of the string, and we now examine one aspect of this influence, governed by the string's torsional dynamics.

We can specify two important dimensionless quantities

relating to torsion: the ratio (Z_{ratio}) of the wave impedance for a torsional wave to that of a transverse wave, and the ratio (S_{ratio}) of torsional wave speed to the transverse wave speed. It is implicit in the work of Schelleng [5], and in the extended discussion of torsional motion by Cremer [13], that these ratios are related by the radius of gyration k:

$$Z_{ratio} = \left(\frac{k}{a}\right)^2 S_{ratio}, \tag{2}$$

where a is the string radius. The quantity $(k/a)^2$ is the second moment of the radial mass distribution, which is governed in manufacturing by the nature of the core material, the wrapping material or materials, and the wrapping technique. (The manufacture's choice of these materials and techniques is also influenced by the fact that the final product must not be too stiff against bending, or the string will be hard to bow because the higher overtones of transverse vibration depart too strongly from a harmonic series [5].)

Figure 8(a) shows the result of simulations in which only the torsional parameters Z_{ratio} and S_{ratio} are varied. S_{ratio} is plotted linearly on the vertical axis, and Z_{ratio} on the horizontal axis. The two boundaries which are apparent as black space with sharp straight boundaries with the coloured pixels are determined, in the lower right, by the physical requirement that $k/a \leq 1$ and, for the upper boundary, by $(k/a)^2 < 0.3$. The former requirement arises from the fact that mass cannot appear outside the physical radius, and the lower boundary represents a guess that manufacturers will not make strings with core density drastically exceeding wrapping density. Calculations were not done outside these boundaries.

We see the familiar mottled appearance of the colours, interspersed with black pixels indicating that Helmholtz motion was still not detected after 100 periods. It is immediately clear that these two torsional parameters exert a significant influence on the playing behaviour of the string. In so far as the figure shows a slight indication of horizontal striation, it appears that the torsional wave speed plays a larger role than the torsional impedance. This might arise because the precise timing of torsional reflections relative to transverse reflections can influence stick–slip transitions, perhaps in a rather sensitive way.

To explore the implications of string manufacture more thoroughly, extensive tests were made over a wide range of bowing forces. The result of another run, at four times the force of figure 8(a), is shown in figure 8(b). Here all simulations that achieved Helmholtz motion in 100 periods are coloured red; the rest are coloured white, except for a limited set which are coloured black. Those pixels mark the positions in this plane of a set of strings on which detailed measurements of string parameters and maximum bow force were made by one of the authors [12]. Their positions on this illustration give some practical meaning to the scales chosen. There are four strings that are homogeneous: two steel E strings and two gut D strings. They lie on a straight line terminating at the upper right. The other black pixel near the top is for a steel-core E string wrapped with aluminium. The four homogeneous strings have $(k/a)^2 = 1/2$, as required by a calculation in elementary mechanics. The other six strings turn out to lie on a straight line with slope $(k/a)^2 = 0.73 \pm 0.05$. They are all D strings, produced by three manufacturers, with one silver and one aluminium wrapping each. The cores included both gut and Perlon. One might speculate that the makers were striving for, and independently achieved, a certain excellence in string quality that ended them all at the same radial mass distribution, but it is apparent from the figure that these strings will behave differently under the bow because of their different torsional properties.

The horizontal gaps in figure 8(b) show that certain values of S_{ratio} do not readily support Helmholtz motion at the normal frequency, at least with this rather large bow force and particular value of bowing position. This suggests effects of the timing of torsional reflections, hinted at above. These are the subject of a continuing investigation.

5. Conclusions

The bowed-string instruments are a rather extreme case of the wide family of sustained-tone acoustic instruments. For any of these, it is becoming possible to perform computer simulations that show effects of sufficient subtlety to be of interest to a skilled player. This inevitably requires the specification of a large number of parameters to describe the physical instrument, and also of parameters to describe the (time-varying) control exercised by the player. The challenge is to find a way through these complexities so that such simulations can shed light on the abiding mysteries of what makes for excellence in the construction of an instrument, or in the performance upon it. The studies described here show that such issues can now be tackled for the bowed-string instruments, and one may hope for significant progress in the coming few years.

The commercial uses of the basic ideas, as described in [18], have already achieved a musical usefulness. However, the problems faced in producing musically useful sounds in real time, controlled by a keyboard, are largely of an algorithmic nature in computer science, and of a hardware nature in electronic engineering. Ultimately, to achieve real-time performer control of such instruments will require an interface capable of the degree of control that the acoustic instruments, with several centuries of development in the case of the bowed strings, have already made available to the most highly skilled musicians. It will be interesting to watch the development of that interface and to compare it with the existing instruments.

However, the main interest in pursuing physical modelling of bowed strings by computer is not to fuel the commercial music industry. Our motives combine natural scientific

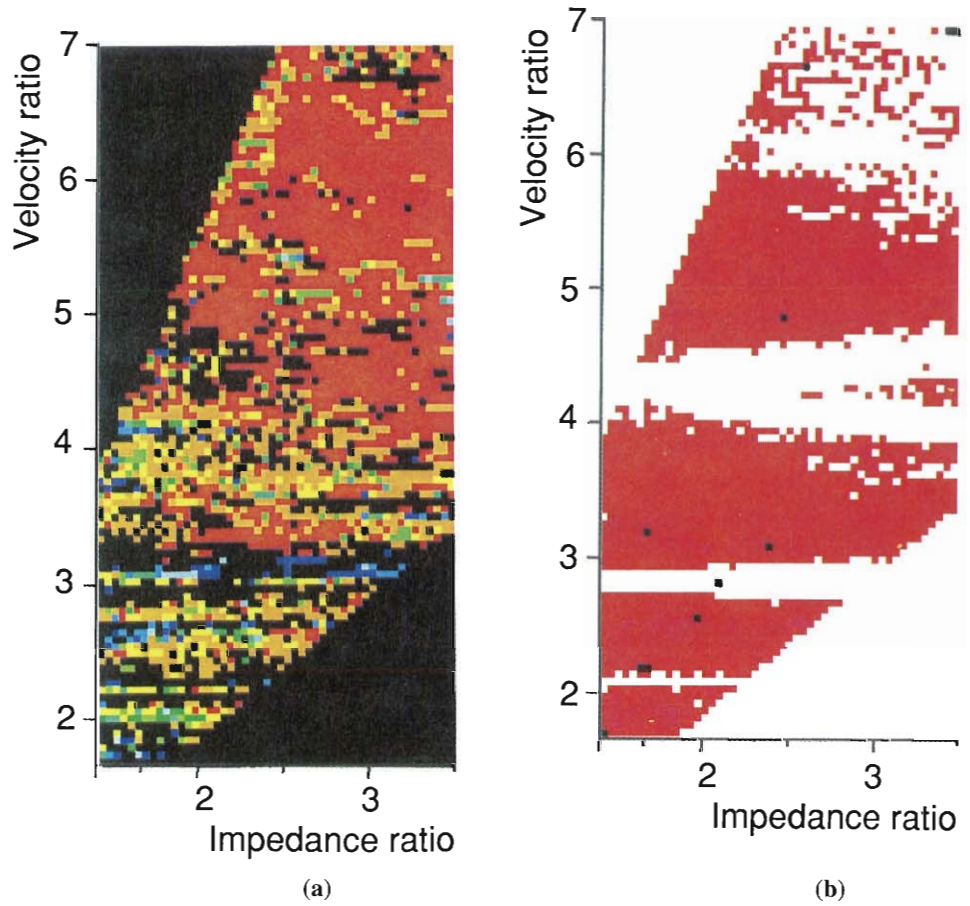

Figure 8. (a) Vertical axis (100 pixels): ratio S_{ratio} of the speed of torsional waves to transverse waves. Horizontal axis (50 pixels): ratio Z_{ratio} of torsional wave impedance to transverse wave impedance . The pixel colour values are as in figure 6(a). The black pixels below and to the right of the coloured region, and above and to the left of the coloured region, demarcated by straight lines, are for values of the ratios for which no simulations were made (see text). Black pixels within the body of the coloured region indicate that Helmholtz motion was not achieved in 100 nominal periods. The bow force in this figure was 10, and bow velocity 1 in the reduced simulation units. (b) Axes as (a), with bow force 40 in reduced simulation units. The red pixels now simply indicate those simulations that achieved Helmholtz motion within 100 periods. The black pixels indicate the parameter values of several real strings, as reported in reference [12]. The straight line connecting the black pixels that terminates in the pair of pixels at the upper right (E strings) represents $Z_{ratio} = (1/2)\, S_{ratio}$, the appropriate value for homogeneous strings. Another E string, aluminium wrapped on steel, is indicated towards the top left of the coloured region. The remaining six strings are all wrapped D strings from three manufacturers and show a remarkable unanimity of choice: $Z_{ratio} = 0{\cdot}73 S_{ratio}$.

curiosity with a desire to have some technological impact on the understanding and manufacture of instruments and their components. Perhaps with better understanding, it will become possible to achieve consistently good playing qualities in relatively cheap student violins. A more immediate hope concerns one particular component of these ancient instruments that has consistently changed with technology: the nature of the strings. It can be hoped that, if the existing models are sufficiently realistic, they will provide a new basis for string design that has up until now been based on trial, error and experience. Computers that are fast enough and running models that are accurate enough can eventually be expected to test strings as yet unmade with equal facility and accuracy to the trials of a skilled player. Computer-aided design will then have come to one part of the ancient art of making violins.

Acknowledgements

The simulations for this paper were done on a Thinking Machines CM2 and on a DEC Alpha computer, both operated by the Pittsburgh Supercomputing Center. The work of one of the authors (R.T.S.) was partially supported by a grant from the National Science Foundation.

References

[1] Previn, A., 1993, *No Minor Keys: My Days in Hollywood* (New York, Doubleday), p. 33

[2] Helmholtz, H., 1954, *On the Sensations of Tone* (New York, Dover Publications), pp. 80–88 (English translation of German edition of 1877).

[3] McIntyre, M. E., Schumacher, R. T., and Woodhouse, J., 1981, Aperiodicity in bowed string motion, *Acustica*, **49,** 14.

[4] Schumacher, R. T., 1994, Aperiodicity, subharmonics and noise in bowed string instruments, *Proceedings of the Stockholm Music Acoustics Conference*, Royal Swedish Academy of Music Publication No. 79 (Stockholm: Royal Swedish Academy of Music), p. 428.

[5] Schelleng, J. C., 1973, The bowed string and the player, *J. Acoust. Soc. Am.*, **53,** 26–41.

[6] Raman, C. V., 1918, On the mechanical theory of vibrations of bowed strings, *Indian Assoc. Cult. Sci. Bull.*, **15,** 1–151.

[7] Pitteroff, R., 1994, Modelling of the bowed string taking into account the width of the bow, *Proceedings of the Stockholm Music Acoustics Conference*, Royal Swedish Academy of Music Publication No. 79 (Stockholm: Royal Swedish Academy of Music), p. 407.

[8] Guettler, K., 1994, *Catgut Acoustical Soc. J.*, November, 8–14.

[9] Rothstein, E., 1994, Review of a concert by Mari Kimura, *New York Times*, 21 April.

[10] McIntyre, M. E., Schumacher, R. T., and Woodhouse, J., 1983, On the oscillations of musical instruments, *J. Acoust. Soc. Am.*, **74,** 1325–1345.

[11] Smith, J. H., 1990, Stick–slip vibration and its constitutive laws, Doctoral dissertation, University of Cambridge.

[12] Schumacher, R. T., 1994, Measurement of some parameters of bowing, *J. Acoust. Soc. Am.*, **96.**

[13] Cremer, L., 1984, *The Physics of the Violin* (Cambridge, Massachusetts: MIT Press).

[14] Woodhouse, J., 1993, On the playability of violins. Part 1: Reflection Functions, *Acustica*, **78,** 125–136.

[15] Woodhouse, J., 1993, On the playability of violins, Part 2: Minimum bow force and transients, *Acustica*, **78,** 137–153.

[16] Woodhouse, J., 1994, Stability of bowed string motion, *Acustica*, **80,** 58–72.

[17] Woodhouse, J., 1993, Idealised models of a bowed string, *Acustica*, **79,** 233–250.

[18] Marans, M., 1994a, The next big thing, *Keyboard Mag.*, February, 100–116; Rideout, E., 1994b, The Yamaha VL1 virtual acoustic synthesizer, *Keyboard Mag.*, June, 104–108; Roads. C., 1994c, Physical modeling, *Keyboard Mag.*, September, 89–103.

[19] Woodhouse, J., 1991, Physical modelling of bowed strings, *Comput. Music J.*, **16,** 43–56.

[20] Schumacher, R. T., and Woodhouse, J., 1995, *Chaos* (to be published).

[21] Gillan, F. S., and Elliott, S. J., 1989, Measurement of the torsional modes of vibration of strings on instruments of the violin family, *J. Sound Vibr.*, **130,** 347–351. 22. McIntyre, M. E., and Woodhouse, J., 1979, Fundamentals of bowed-string dynamics, *Acustica*, **43,** 93–108.

Robert T. Schumacher is Professor of Physics at Carnegie–Mellon University, where he has been on the faculty since 1957. Since 1975 he has concentrated his research interests to musical acoustics, particularly oscillation mechanisms and the simulation of oscillations in sustained tone instruments. Before 1975 he worked in magnetic resonance, particularly nuclear magnetic resonance in solids. He is the author of an introductory undergraduate text *Magnetic Resonance* (New York: W. A. Benjamin) published in 1970. He has been a Sloan Foundation Fellow and a National Science Foundation Senior Post-Doctoral Fellow, and is a Fellow of the American Physical Society.

James Woodhouse is a Reader in the Department of Engineering at Cambridge University. After an undergraduate career in mathematics at Cambridge, an interest in violin making led him to work on violin acoustics for his doctoral studies. After an interlude with a scientific consultancy firm working on more mainstream problems in noise and vibration, he joined the staff of the Department of Engineering in 1985 and was able again to direct part of his research effort towards the fascinating but frustrating problems of musical instruments.